

1 **Distribution and migration of deep-water hake (*Merluccius***
2 ***paradoxus*) in the Benguela Current Large Marine Ecosystem**
3 **examined with a geostatistical population model – a preview**
4 *****

5
6 Teunis Jansen^{1,5}, Kasper Kristensen⁵, Uffe Høgsbro Thygesen⁵ and Jan E. Beyer⁵

7
8 1) BCC – Benguela Current Commission, Private Bag 5031, Swakopmund, Namibia.

9 2) MFMR – Ministry of Fisheries and Marine Resources, PO Box 912, Swakopmund, Namibia.

10 3) DAFF – Department for Agriculture, Forestry & Fisheries, Cape Town, South Africa.

11 4) Institute of Marine Research, P.O. Box 1870 Nordnes, N-5817 Bergen, Norway.

12 5) DTU AQUA – National Institute of Aquatic Resources, Charlottenlund, Denmark

13 6) Rhodes University, Department of Ichthyology and Fisheries Science, P.O. Box 94, Grahamstown
14 6140, South Africa

15 Corresponding author: Teunis Jansen; DTU AQUA - *National Institute of Aquatic Resources, Technical*
16 *University of Denmark; Charlottenlund castle, 2920 Charlottenlund, Denmark; Tel.: +4530667840; Fax:*
17 *+4533963333; E-mail address: Tej@aqu.dtu.dk.*

18
19 *** Disclaimer #1:** This study is *in progress*. The results are not final, so they should not be used outside
20 the EcoFish phase II workshop.

21 *** Disclaimer #2:** Following scientists are contributing to this study: Paul Kainge², Deon Durholtz³, Tore
22 Strømme⁴, Marek Lipinski⁶, John Kathena², Margit Wilhelm^{1,5}, Tracey Fairweather³, Sarah Paulus², Henrik
23 Degel⁵, Hashali Hamukuaya¹

24 Abstract

25 Deep-water cape hake (*Merluccius paradoxus*) is of primary ecological and economic importance in the
26 Benguela Current Large Marine Ecosystem in South Africa and Namibia. The assessment and
27 management is done for two separate stocks, assuming no transboundary movements and no spatial
28 population patterns within each stock area (country). Results from single transboundary surveys have
29 indicated that this is not likely to be true. In the present study, we combine data from multiple demersal
30 trawl surveys from the entire Benguela large marine ecosystem to estimate spatial and temporal
31 distribution patterns of *M. paradoxus*. We follow the natal homing hakes from 0.5 to 7.5 years of age as
32 they form three main spatial trends. From the centrally located nursery area on the African south-west
33 coast, they initiate their migration in their second year. The resident hakes stay or move up to 3-400 km
34 south or north, only to return in their third or fourth year. The migratory hakes migrate up to 1200 km
35 either north or south-east and return at the age of 6+ years. The alongshore migrations are combined
36 with migrations towards deeper waters. From the nursery area at 150-250 m depth they move deeper
37 and at the age of 4 most of the hakes are in 350+ m of depth.

38 Our results indicate a transboundary nursery hotspot, as well as transboundary migration of several
39 cohorts. Consequently, assessment and fisheries management could be improved by shifting to an
40 internationally scope.

41 We also suggest that the southern migratory part of the population migrate out of the area covered by
42 the surveys. Incomplete coverage of the stock appears to be a problem for stock assessment; an
43 extension of the survey should therefore be considered.

44 Our analyses were done with a new Latent Cohort GeoPop model – a geostatistical model (aggregated
45 log Gaussian cox process model with correlations). The purpose of this version is to track the cohorts in
46 time and space.

47

48

49

50 Keywords: *Hake, northern Benguela, southern Benguela, Merluccius, paradoxus, transboundary,*
51 *migration, geostatistics, LGC, growth, gear selectivity, South Africa, Namibia, demersal trawl*

52

53

54 Introduction

55 Deep-water cape hake (*Merluccius paradoxus*) is among the most dominant demersal fish species in the
56 South East Atlantic. The species is ecologically important in the Benguela Current Large Marine
57 Ecosystem as an opportunistic predator (mainly fish, including hake) (Botha, 1980; Payne et al., 1987),
58 and as prey for the top predators such as fur seals, cephalopods, sea birds and many demersal and
59 pelagic fish species (Pillar & Wilkinson, 1995). *M. paradoxus* (together with the sympatric shallow water
60 hake *M. capensis*) is also targeted by fisheries throughout its distribution (BCC, 2012). Annual hake
61 landings in Namibia, South Africa and Angola averaged 300,000 tonnes per year in 2000-2010, with
62 nearly 30% being *M. paradoxus* (BCC, 2012). Hakes are the economically most important fish stocks in
63 both Namibia and South Africa, worth about 5 % of the GDP in Namibia (MFMR & NPC, 2013).

64 *M. paradoxus* inhabit the continental shelf slope from around 17°S in Angola/Namibia to about 27°E in
65 South Africa (Payne, 1989). Spawning takes place between 200 and 600 meter depth South and West of
66 South Africa (Jansen & et al., in prep)+other refs. Established views suggest a largely stationary
67 population with some local inshore-offshore movement and weak patterns of geographical hot-spots
68 (Payne & Punt, 1995). However, it has been suggested earlier (Le Clus et al., 2005) that this picture may
69 be inadequate, largely due to sampling limitations. An analysis of DNA microsatellites indicated one
70 panmictic stock (Bloomer et al., 2009). This was confirmed when examining in mtDNA from less than
71 three years old hakes (von der Heyden et al., 2010). However, the mtDNA revealed significant
72 differences between hakes from each side of the Orange River mouth (i.e. national border between
73 Namibia and South Africa) (von der Heyden et al., 2010). The spatial population structure (stock
74 structure) thus remains uncertain and several hypotheses have been proposed. Most recently, an
75 analysis of length distributions from survey catches supported the panmictic view and described
76 alongshore and offshore migrations patterns (Strømme et al., In prep.). Today, the species is assessed
77 and managed separately in Namibia and South Africa (Figure 1).

78 Nearly all studies of the biology and ecology of *M. paradoxus* have been on a local or national scale,
79 even though several decades of high quality research survey data have been collected from demersal
80 bottom trawl surveys throughout its entire distribution area. Regional transboundary analyses on the
81 combined survey data sets (which only recently became available) have not been performed because
82 the data are not directly comparable. The various surveys conducted by the three vessels have used
83 different trawl gear with different catch efficiency. In the present study, we quantify this effect, so we
84 can address the spatial population dynamics with a state-of-the-art integrated geostatistical population
85 model. We develop a new version of the “GeoPop” model, which combines a novel geostatistical
86 approach with a simple population model. The central aim of the study is to analyse the spatial
87 population dynamics. We do this by estimating time series of cohort-specific distributions and map them
88 for examination of putative migration patterns.

89

90 **Materials and methods**

91 *Scientific trawl survey data*

92 *M. paradoxus* were caught during demersal trawl surveys on the continental shelf and slope in the
93 Benguela-Agulhas ecosystem from 17°S in the North, round Cape of Good Hope to 27°E in the west (Fig.
94 1). The surveys are conducted each year in January-May for routine biomass calculations by the Ministry
95 of Fisheries and Marine Resources (MFMR) in Namibia and the Department of Agriculture Forestry and
96 Fisheries (DAFF) in South Africa. No trawl samples were available from Angolan waters due to species
97 identification problems between *M. capensis* and *M. paradoxus* and *M. polli* (Benguela hake, which is
98 largely caught in Angola). Three different trawl gear types were used, each fishing at a different trawl
99 speed or with different size spread or ropes (Table 1). Total catch was weighed and sorted by species.
100 Large catches were subsampled. The weight of the hake catch (separated by species) was recorded and
101 total lengths of individual hake were measured in cm (rounded down). Subsamples were subsequently
102 raised to the total catch.

103 The standardized efficiency of the trawl was compromised by very strong winds in 2002 and 2011 off the
104 South African west coast (Wieland et al, in prep). These stations were therefore removed from the
105 dataset.

106 Catch Per Unit Effort (CPUE) of each length group in each haul was calculated as number per hour
107 trawled. This measure was used as a relative index of hake density.

108 The survey dataset consisted of 7.1 million measures *M. paradoxus* in 7,000 trawl hauls from 1998 to
109 2011. 324 of the hauls were especially informative in relation to gear inter-calibration, because they
110 were taken with different gears, less than 3 hours apart and at a maximum distance of 18 nautical miles
111 (nm). The samples were from the entire region (Figure 1), and they were fairly equally distributed
112 among the years (Figure 2a). Most samples were taken in January-February, while the South African
113 South coast was covered in April-May (Figure 2b). Trawling was predominantly done during the day
114 (Figure 2c). The Gisund trawl was used most frequently (Figure 2d).

115 *The Latent Cohort GeoPop model*

116 A geostatistical model (aggregated log Gaussian Cox process model with correlations) was used to
117 describe the density index of *M. paradoxus* cohorts through space and time, along environmental
118 gradients, observed using various gear types, as the hake recruited, grew and died.

119 Related models have previously proved their value for cod (Kristensen et al., 2013; Lewy & Kristensen,
120 2009) and mackerel larvae (Jansen et al., 2012). However, this new “Latent Cohort GeoPop model”
121 tracks the cohorts. This is not only biologically meaningful, it is also advantageous for the complex and
122 time consuming model fitting algorithm to reduce the number of parameters from 100 length classes to
123 eight year classes. To obtain growth rates independent of otoliths-based age data, we integrated a
124 length-frequency analysis (LFA) in the model complex. The LFA estimates the age distribution of a given
125 length class by following the cohort-peaks in the length frequencies as they grow (Equation 2).

126 We modelled the density index (CPUE) for eight age classes in the period 1998 to 2012. The cohorts
 127 were followed in time steps of one year and in a spatial resolution of 25x25 km. These 135,120 (8 age
 128 classes x 15 years x 1126 grid-cells) random variables were assumed to follow a log Gaussian
 129 distribution, and determine the mean of catch (in numbers), which are assumed to follow a Poisson
 130 distribution, conditional on densities. This model structure is referred to as a log-Gaussian Cox process
 131 model, and has been shown as a good representation of count data from catches that are correlated,
 132 over-dispersed and with many zero-values (Kristensen et al., 2013). The Poisson distribution allows for
 133 zero catches, while the randomness of the density fields imply over-dispersed catches (relative to
 134 Poisson) and in particular many more zero catches than would be found in a pure Poisson model. Finally,
 135 the catches inherit the correlation structure of the density field.

136 A key feature of the model was the utilization of the information that resides in the patchy distribution
 137 of fish. This behavioural element was modelled in three parts: First and second, patchiness in space and
 138 in time on a large scale (correlations between cells) and, third, the tendency of fish to aggregate with
 139 fish in similar sizes on a local scale (within age groups, within trawl hauls, “nugget effect”).

140 The spatial large-scale correlation was assumed to decay with distance and the stability over time of
 141 these patterns was estimated as the correlation from year to year of the density in a given cell.
 142 Temporal correlation decayed exponentially with distance in time (years) and spatial correlation did
 143 approximately the same. However, in order to avoid correlation over land (e.g. the Cape point), we
 144 implemented the spatial correlation effect as a Gaussian Markov random field. To present the
 145 parameter estimates of these correlations in a meaningful way, we expressed the distance (H) and de-
 146 correlation time (T), as the distance in space and in time where the correlations have decayed to e^{-1}
 147 (explaining approx. 14% of the variance). Documentation of these correlation structures were published
 148 in Kristensen et al. (2013).

149
 150 The third relation in the model that should reflect fish behaviour was the “nugget effect”. Catches of
 151 certain fish sizes tend to be over-represented in trawl hauls compared to the size distribution in the
 152 sampled population. This may be due to size structured aggregations (schools) or because the local
 153 habitat favours fish of a certain size e.g. through the available type of food. This local effect was
 154 accounted for by estimating the age-class specific variation in the hauls (σ_N^2).

155 A simple population model related the cohort abundance index from one year to the next, by estimating
 156 the mean recruitment (N_0) and mean total mortality (Z). These processes were assumed to be
 157 independent of space and time. The mean total mortality was modelled as a constant corresponding to
 158 the exponential decay model:

$$159 \quad N_t = N_0 e^{-\bar{Z}\Delta t},$$

160 where N_t was the abundance after the mortality \bar{Z} (year^{-1}) in Δt time steps (in years)

161 We linked the observations by length to cohorts, by a size spectrum analysis. This part of the model
 162 followed the cohort signals as abundance peaks that grew up through the size spectrum. For simplicity,
 163 we assumed that the size distribution the individual fish in a cohort is given by a Gaussian density with a
 164 mean determined by a von Bertalanffy growth model:

$$165 \quad L = L_{inf} (1 - e^{-K(a-t_0)}),$$

166 where L is the mean length in cm at age class a (years), L_{inf} (cm) the mean length of infinitely old fish,
 167 i.e. the asymptotic length at which growth is theoretically zero, K (Year⁻¹) is the rate at which L
 168 approaches L_{inf} and t_0 (years) is the x-axis interception, i.e. a theoretical age at length 0 cm.

169 The standard deviation of the Gaussian distributed individual lengths around the mean length at age
 170 was assumed to increase linearly with age with $\sqrt{\sigma_{rate}^2}$ from the initial standard deviation $\sqrt{\sigma_{init}^2}$.

171 The first cohort peak was assigned an age of 0.5 years, ...

172 Finally, the catch is affected by the catchability of the gear and this effect was implemented as

$$173 \quad SF_G = \gamma (1 + 3^{-(2/SR_G)(L-L50_G)})^{-1},$$

174 where SF is the selection factor, γ is the efficiency factor, SR is the selection range and $L50$ is the fish
 175 length (cm) at half selection for three different gear types G .

176 The parameters in the model were estimated using the maximum likelihood principle based on the
 177 Laplace approximation and thus the estimation follows the principles of Kristensen et al. (2013).
 178 However, the present model was more challenging due to non-convexity issues of the aggregated log
 179 Gaussian Cox process and the much larger area and amount of data - see details in Supplementary
 180 information 2. When possible, we followed the parameter notation of Kristensen et al. (2013). A more
 181 concise documentation of the present model was furthermore given in Supplementary information 1.

182 The fitted model was finally used to calculate annual estimates of the relative index of hake density
 183 (CPUE) for each cohort in each age class (0.5-7.5) in each 25 x 25 km cell. These spatiotemporal
 184 distribution patterns were also transformed into a more meaningful coastline-oriented coordinate
 185 system. This was done by projecting the estimated abundances in the Cartesian coordinate system onto
 186 a curvilinear axis following the coastline from Port Elizabeth on the South-African south coast to the
 187 Namibia-Angola border (Kunene River) in the North (see Fig. 1). The shortest distance to any point on
 188 the coastline, as defined in the R package "mapdata" (Becker et al. 2013), was used. The same coastline
 189 definition was used for all maps (Figure 1).

190

191 Results

192 The model was fitted to the catch data and the parameter estimates are given in Table 2. The fitted
 193 model explained 67% of the variation in the data. However, it was not possible to estimate the
 194 uncertainties of the parameters using the standard approach, because of an irregularity in the likelihood
 195 surface. ***[Disclaimer #3: This is the challenge we are addressing at the moment. The estimation
 196 problem mainly affects the gear selectivity. The distribution-maps are to a large extent OK, however,
 197 the overall density estimates, especially Namibia vs. South African south coast are not scaled correctly
 198 yet. We have therefore removed text and figures about the gear effect and growth. The rest is given
 199 for the user to understand the approach and get an understanding of the information that will be
 200 provided in the final peer reviewed paper].***

201 The resulting standard errors of the parameter are given in Table 2.

202 *Spatial patterns (distribution, migration and population structure)*

203 The relative index of hake density (CPUE) was estimated by year and age class in each of the grid-cells
 204 throughout the study area. The hake densities were found to be spatially correlated with a spatial de-
 205 correlation distance (H) of 268 km. [spatial variance]. The local abundance varied substantially from haul
 206 to haul, with a CV of 70% (nugget effect). The spatial patterns of the cohorts were found to be fairly
 207 stable with a temporal de-correlation period (T) spanning 2.4 years. We illustrated the main trends in
 208 age specific distributions by mapping the average spatial distributions of the six cohorts that the model
 209 could follow from the ages of 0.5 to 7.5 years (Figure 3-7). These average distributions were then used
 210 to infer putative migrations through their life. We analysed the alongshore and the off-shore (depth)
 211 migration separately.

212 For scrutiny of alongshore migration patterns, we projected the distributions onto a curvilinear axis
 213 following the coastline from Port Elizabeth in the south-east to the Namibia-Angola border (Kunene
 214 River) in the North. The resulting alongshore distributions were then plotted by age for each cohort
 215 (Figure 5-9) and for the average of all cohorts (Figure 7-11). The 0.5 year old recruits were concentrated
 216 in an elongate retention area from Cape point to 50 km north of the Orange River mouth. Highest
 217 densities were found north of the Olifants River mouth (Figure 3 and Figure 7). This initial pattern was
 218 preserved well into the second year, after which, *M. paradoxus* began an alongshore redistribution
 219 (Figure 7-11). From the age of 2.5 years, the distribution was clearly different than the recruit
 220 distribution, showing that the recruits had spread out. This developed into a broad resident patch at the
 221 nursery area, divided from a northern and an eastern migrating patch. They reached their outermost
 222 positions at the age of 4.5, after which they slowly returned. However, the southern migrating patch on
 223 the South African south coast disappears between the age of 4 and 6, close to the edge of the surveyed
 224 area (around 27°E). These patterns were illustrated by adding the movements of the centre of gravity
 225 (CoG) on each side of Orange River mouth and Cape good hope onto Figure 8 (grey dashed lines). We
 226 estimated the south-eastern CoG between the age of 4 and 6 by assuming an annual alongshore
 227 movement at the same distance as observed in the northern migration. At the age of 5, the
 228 northernmost observed hakes had migrated at least 1200 km and the CoG had reached a distance of 750

229 km to the Orange River. In total, the hakes have moved up to 2400 km alongshore in 7.5 years, assuming
 230 a complete return migration. The alongshore migration was combined with migration towards deeper
 231 waters (Figure 9). At the age of 6.5, where 99 % of *M. paradoxus* are mature (Singh et al., 2011), the
 232 migrating components of the population seemed to have returned to the spawning area (Jansen & et al.,
 233 in prep). The depth distribution was narrower towards the south (Figure 9). We could thus confirm the
 234 well-known offshore migration to deeper waters with age (Figure 10) and expand the understanding of
 235 the depth migration by showing systematic spatial differences.

236 The distribution maps and plots showed that the border between Namibia and South Africa, presently
 237 used to separate *M. paradoxus* stocks, is in a high density nursery area. The national border did not
 238 coincide with any discontinuity of the recruit distribution (Figure 7). Examination of the distribution
 239 changes through the first 4 years of life of each year class indicated transboundary movements of the
 240 year classes 1998, 1999 and 2000. Transboundary migration may very well have taken place every year
 241 since then, but this is not clearly reflected in the distribution sequences.

242 The double-sided return migration clearly demonstrates natal homing, but with an unknown precision.
 243 Furthermore, a large part of the population seemed to be more resident “resident” with none or short
 244 migrations in relation to the nursery and spawning area.

245 *Abundance time series*

246 CPUE time series of the recruits were calculated for each area (Figure 11a). The overall annual
 247 recruitment increased substantially from a relatively low level in 1998-2002, to a higher level in 2003-
 248 2011. The recruitment was relatively stable in each of these periods. The increase in recruitment was
 249 followed by an increase in larger *M. paradoxus* (Figure 11c).

250

251 **Discussion**

252 *The GeoPop Model and its fit to the observations*

253 | The finding of a ridge in the likelihood surface lead to some concern whether the fitting procedure had
 254 found the global optimum. The reliability of the estimates was therefore tested by selecting “true”
 255 parameters for a virtual population example. The population was then sampled and the parameters
 256 were estimated from the samples. This demonstrated that the original parameters could be re-
 257 estimated despite of the irregularity of the likelihood surface. This test was documented in
 258 Supplementary information 2.

259 [ToDo: temporal variance age vs. cohorts in space]

260 *Spatial patterns (distribution, migration and population structure)*

261 Maps and plots of the distribution of *M. paradoxus* were created as age explicit overviews for the entire
 262 Benguela large marine ecosystem. The most parsimonious change from one age distribution to the next
 263 clearly indicated ontogenic migration patterns of the juvenile and adult hake.

264

265 The migration patterns are generally in agreement with the results presented in Strömme et al. (in
 266 prep), but with some differences:

- 267 1. We find the 0.5 years old recruits in an elongate retention area from Cape point to 50 km north
 268 of the Orange River mouth, while Strömme et al. (in prep) found one central nursery area
 269 between Hondeklip Bay and Orange Banks.
- 270 2. Strömme et al. (in prep) found an initial coastward migration of 10-15 cm fish, which did not
 271 appear in our results. This coastward migration could have been missed due to our annual time
 272 steps. This was similarly missed in a GeoPop analysis of migration of *M. capensis* (Jansen & et al.,
 273 In prep.).
- 274 3. [Tore/Marek, could you please add other differences, if any, to this list]

275

276 Furthermore, our findings suggest that the Southern migrating subpopulation moves, either vertically or
 277 horizontally, out of the area covered by the South African south coast survey. The subpopulation
 278 disappeared close the eastern edge of the survey area only to reappear two years later. The
 279 disappearance coincides with the age where the northern migrating hakes are at the greatest distance
 280 from the nursery/spawning, thus strongly suggesting that the disappearance is due to eastern migration
 281 out of the survey area. Therefore, we recommend that the South Africa south coast survey be extended
 282 at least 600 km to the east in order to cover the main distribution of the 4-6 year old eastern migrating
 283 hakes. This corresponds approximately to 30°E outside Durban. The disappearance of the 4-6 year old
 284 eastern migrating hakes corresponds to an unexplained drop in south coast survey selectivity in the
 285 assessment of *M. paradoxus* (Rademeyer & Butterworth, 2013). If this hypothesis is verified, then the
 286 assessment model should feature an estimation of the missing hake.

287 A similar problem with insufficient depth coverage of the surveys has been raised in the literature. While
 288 the Namibian survey has covered the area down to 6-700 m, the South African west coast survey has
 289 missed substantial parts of the population of larger fish because the survey only fished down to 500 m
 290 before 2011 (Wieland et al. in prep).

291 In our treatment of the spatial patterns, we presented annual snapshots of austral summer
 292 distributions. Seasonal migration patterns were not included. Such seasonal movements have been
 293 suggested as annually repeated inshore-offshore movement of hake in South African waters (Millar,
 294 2001), with the offshore movement happening in winter where the *M. paradoxus* is known to spawn
 295 (Jansen & et al., in prep)+other refs.

296 The indication of transboundary migrations between South Africa and Namibia, suggests that
 297 assessment and management can be done more optimal internationally than nationally. A new
 298 assessment approach could also consider explicit modelling of the large scale pattern of resident versus
 299 migratory parts of the population. These three temporary subpopulation units could be growing at
 300 different rates. Most likely also experience different natural and fisheries mortality rates in the years
 301 when they are semi-separated. Accounting for these dynamics in a transboundary integrated stock

302 assessment model that includes hake size-species interactions, may provide management advice closer
303 to the maximum the sustainable yield (MSY).

304

305 **Conclusion**

306 [See abstract]

307

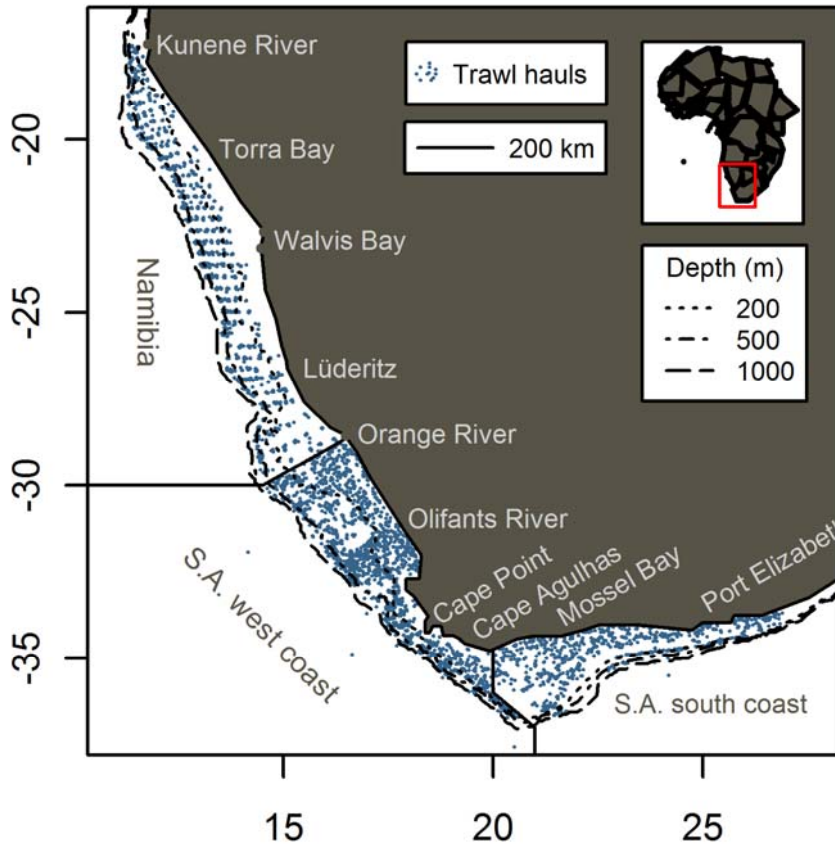
308 **Acknowledgements**

309 We wish to thank the lab and field assistants from NatMirc (Namibia), DAFF (South Africa) and Norway
310 that sampled and measures the many hakes analyzed in the present study. The sampling was funded by
311 MFMR (Namibia), DAFF (South Africa) and Norway. Data analysis and publishing was funded by
312 EuropeAid through the EcoFish project (CRIS Number C-222387).

313

314 **Figure legends**

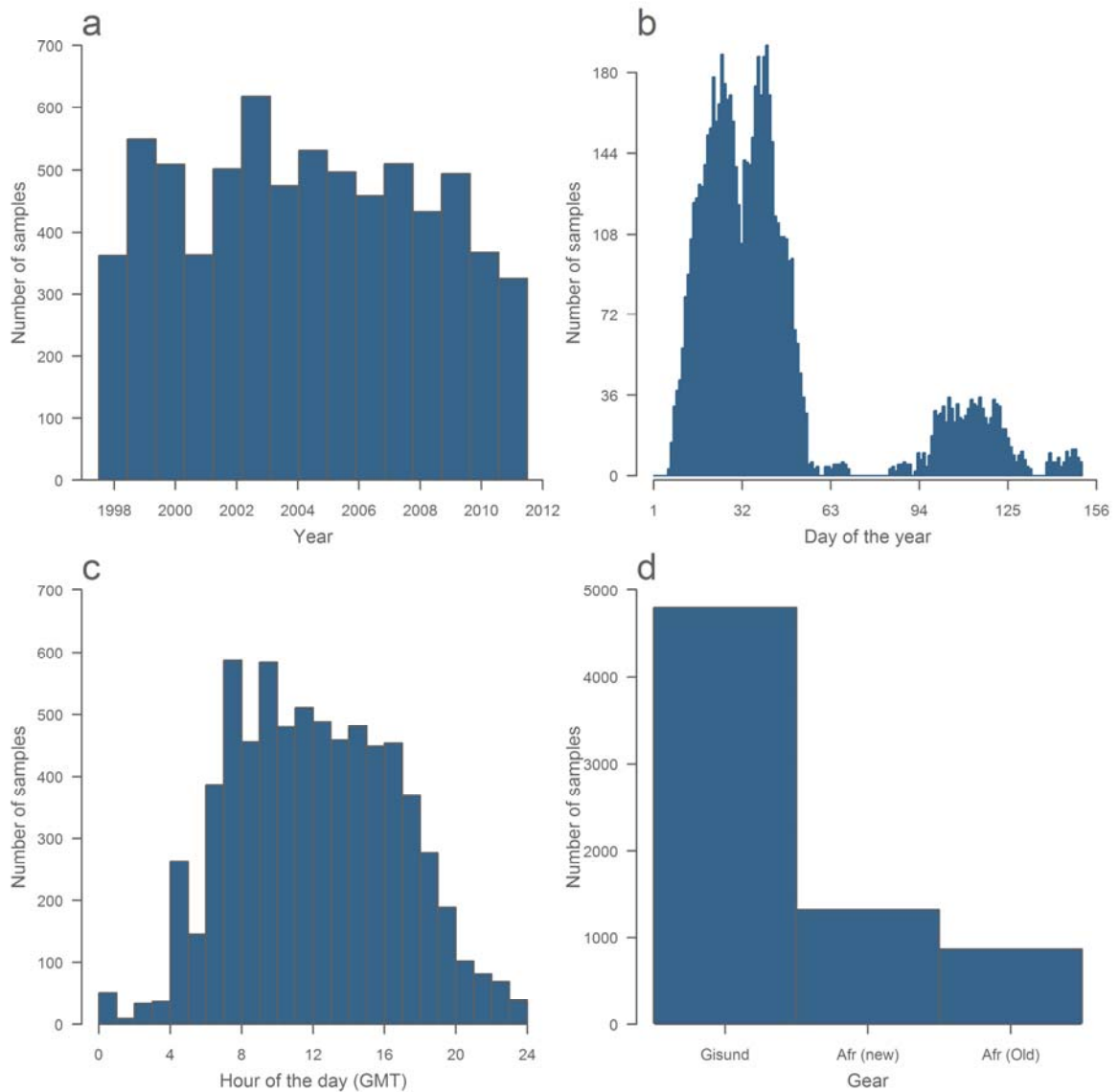
315



316

317 Figure 1. Map of study area with sample locations (dots), isobaths and place names referred in the text.

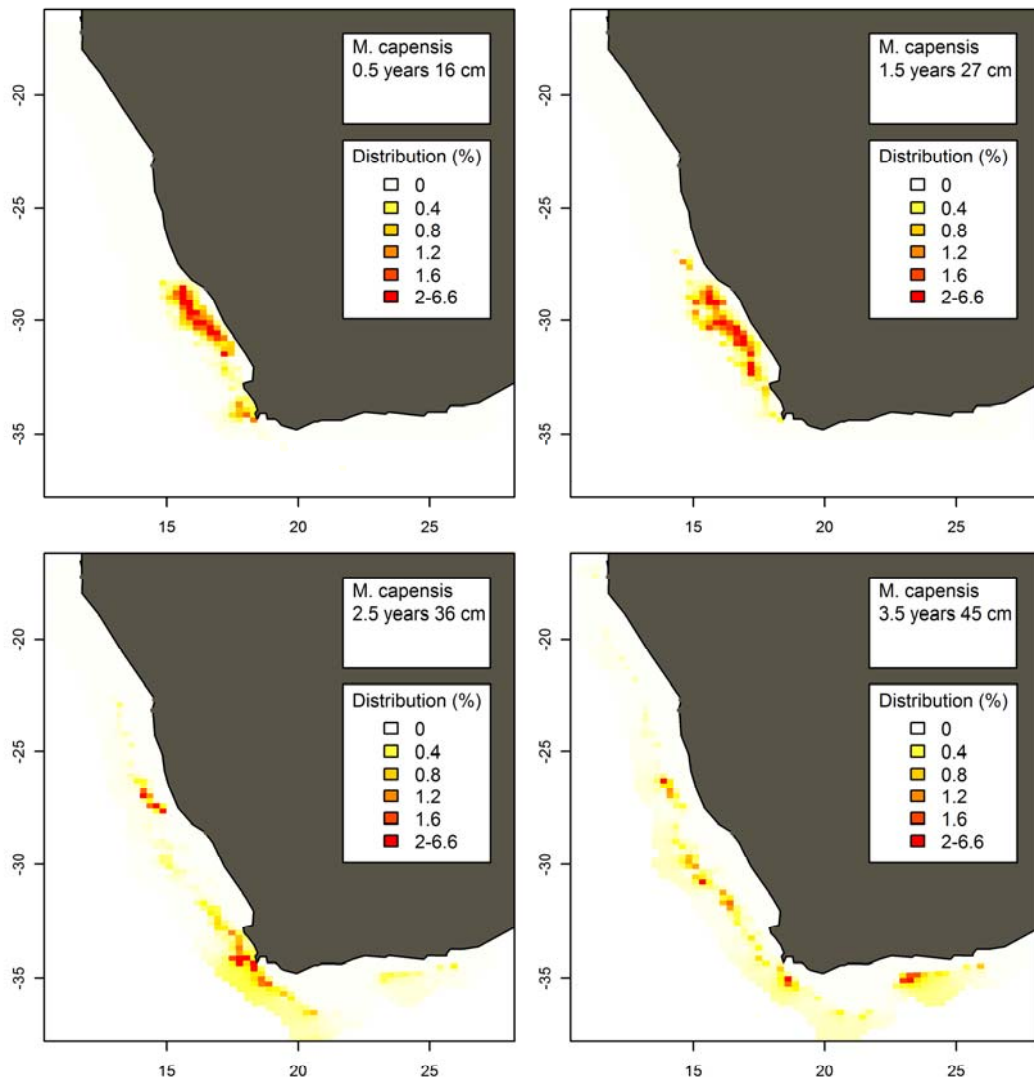
318



319

320 Figure 2. Bottom trawl survey samples (trawl hauls) from 1998-2011 in the studied area. Number of
 321 samples by a) year. b) ordinal day. c) hour of the day. d) gear type.

322

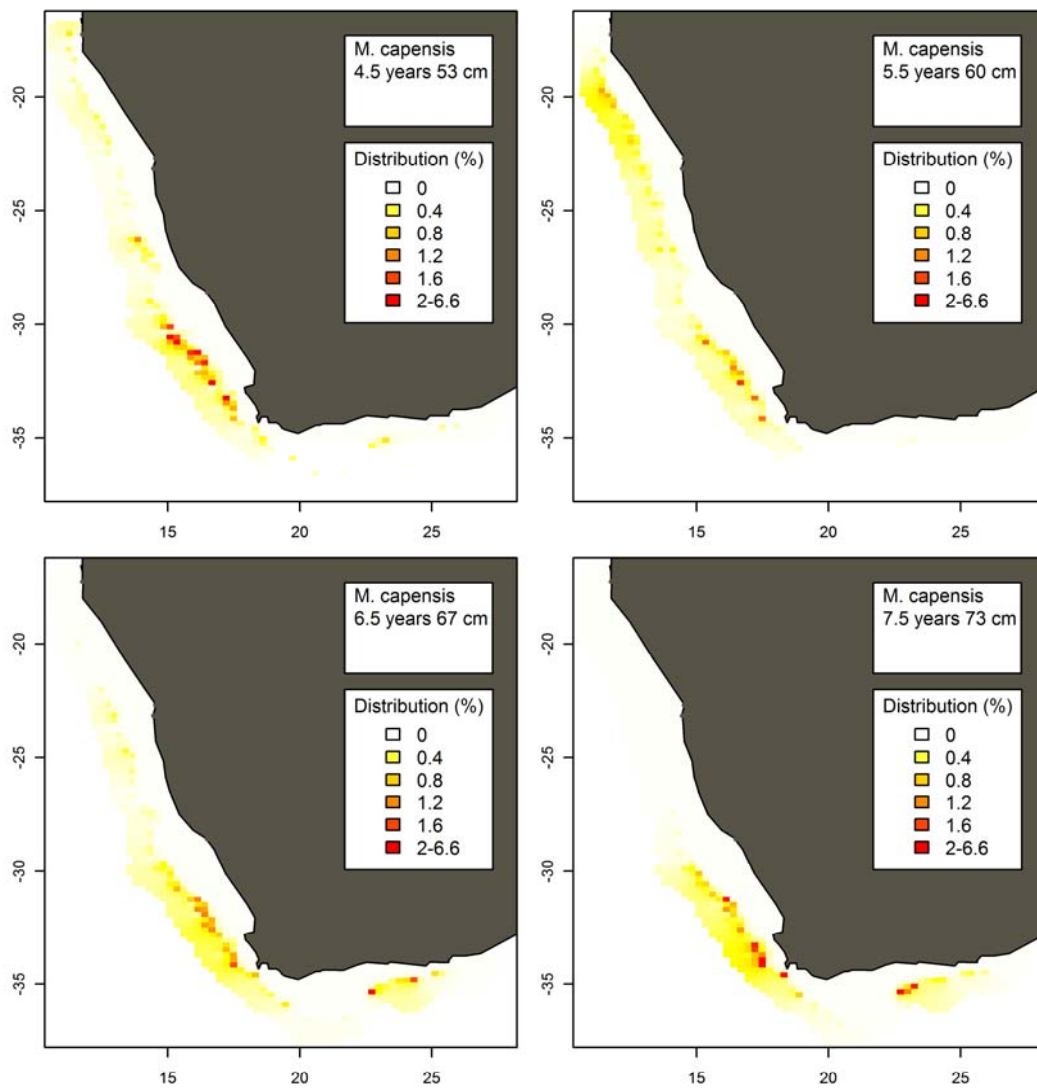


323

324 Figure 3. Distribution maps of deep water cape hake (*M. paradoxus*) by age. a) 0.5 years. b) 1.5 years. c)

325 2.5 years. d) 3.5 years.

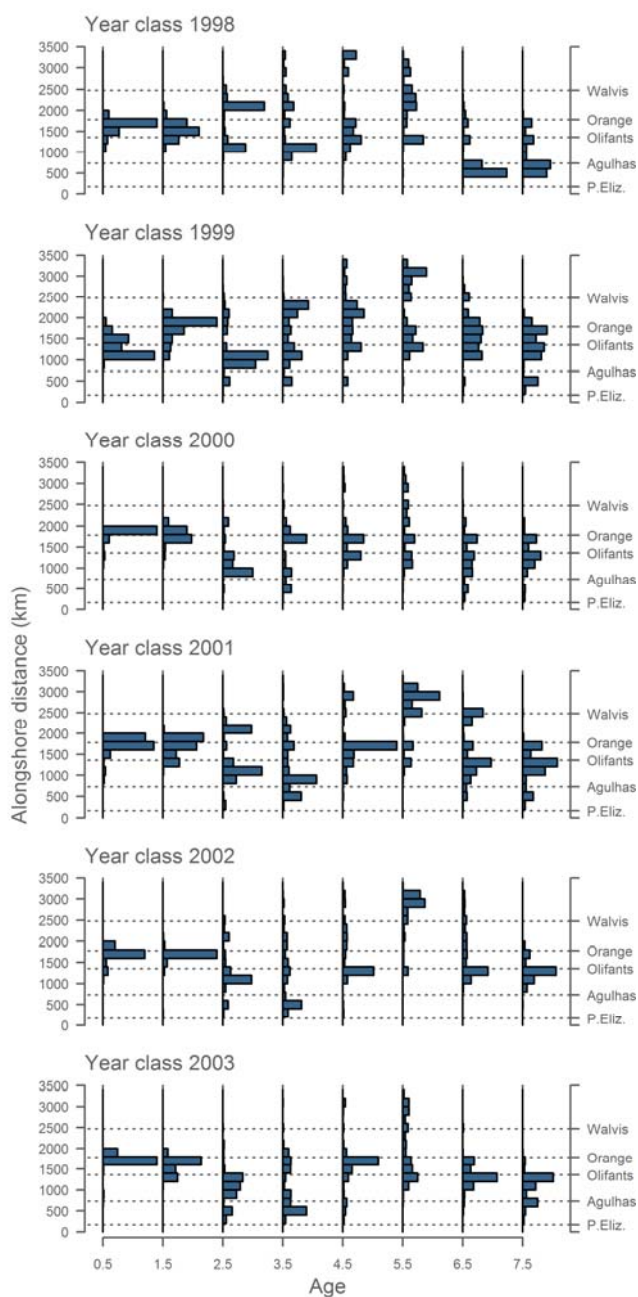
326



327

328 Figure 4. Distribution maps of deep water cape hake (*M. paradoxus*) by age. a) 4.5 years. b) 5.5 years. c)
329 6.5 years. d) 7.5 years.

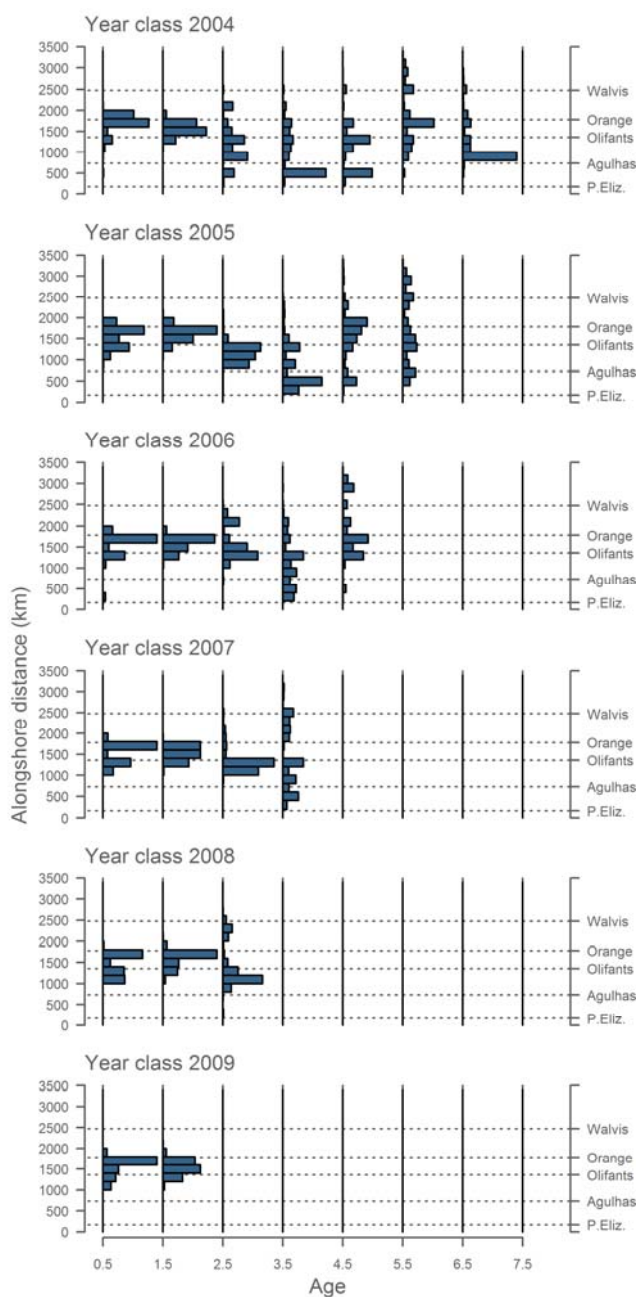
330



331

332 Figure 5. Alongshore distribution in number of fish by age for cohorts 1998-2002 of deep water cape
 333 hake (*M. paradoxus*). The spatial distribution has been projected onto a curvilinear axis following the
 334 coastline from Port Elizabeth in the south-east to the Namibia-Angola border (Kunene River) in the
 335 North.

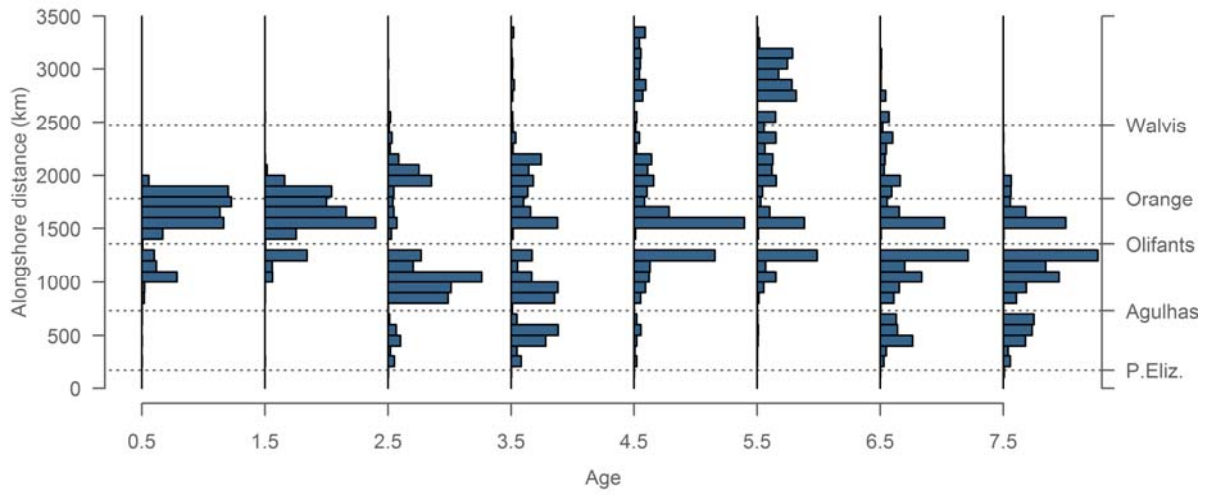
336



337

338 Figure 6. Alongshore distribution in number of fish by age for cohorts 2004-2008 of deep water cape
 339 hake (*M. paradoxus*). The spatial distribution has been projected onto a curvilinear axis following the
 340 coastline from Port Elizabeth in the south-east to the Namibia-Angola border (Kunene River) in the
 341 North.

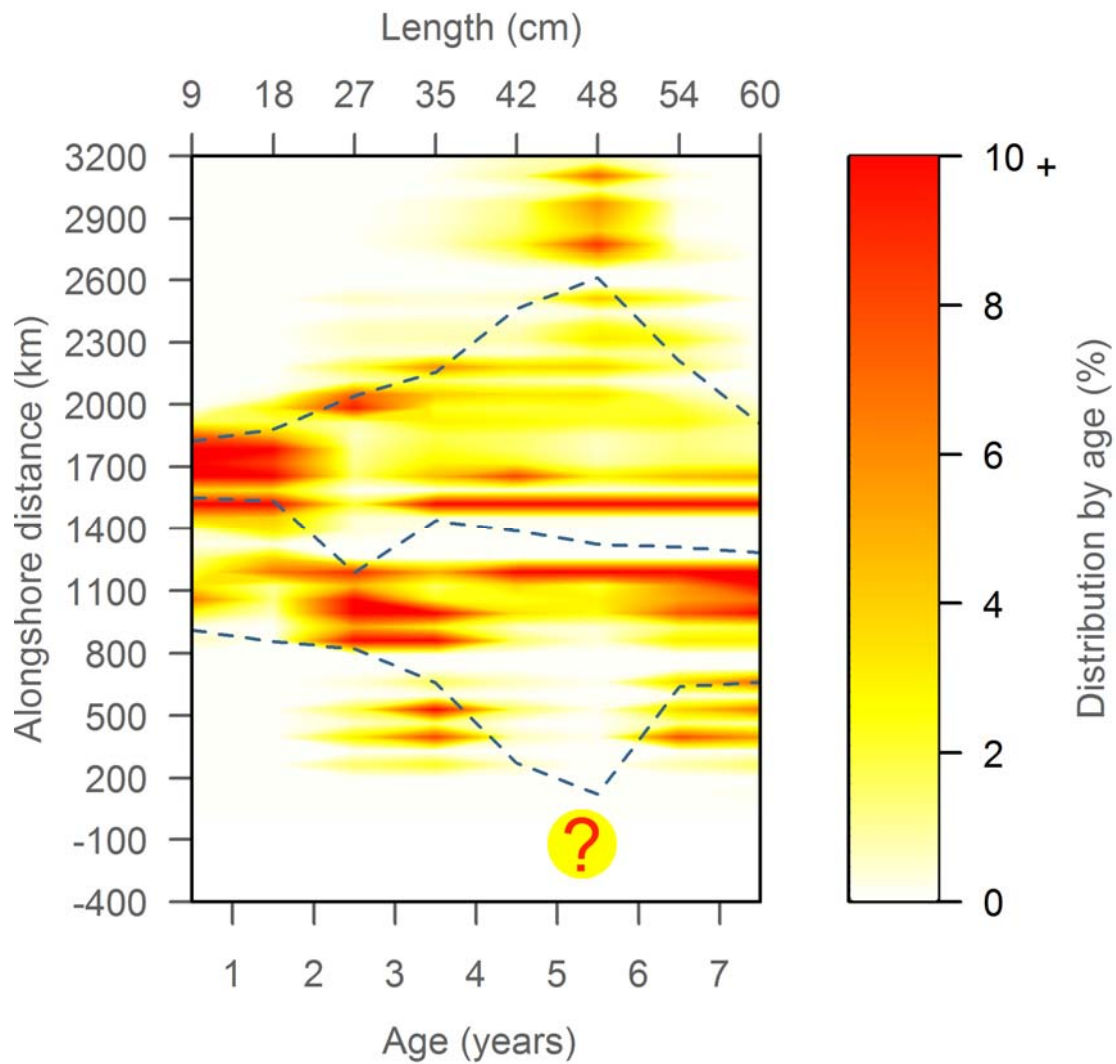
342



343

344 Figure 7. Alongshore distribution by age of deep water cape hake (*M. paradoxus*). Average of all year
 345 classes. The spatial distribution has been projected onto a curvilinear axis following the coastline from
 346 Port Elizabeth in the south-east to the Namibia-Angola border (Kunene River) in the North.

347

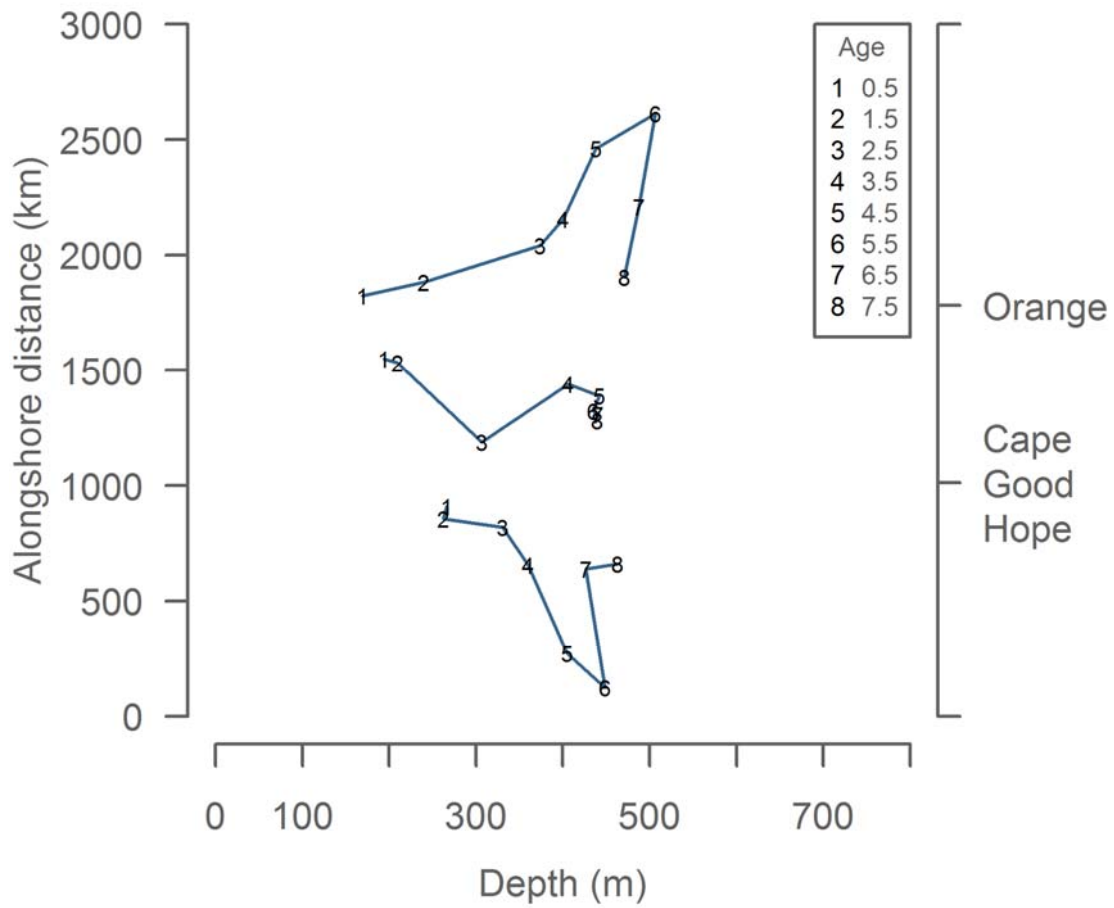


348

349 Figure 8. Alongshore distribution of deep water cape hake (*M. paradoxus*) by age and mean length. The
 350 Centre of Gravity is indicated by grey dashed lines for hakes north of 2150 km and south of 1550 km.

351 The spatial distribution has been projected onto a curvilinear axis following the coastline from Port
 352 Elizabeth in the south-east to the Namibia-Angola border (Kunene River) in the North.

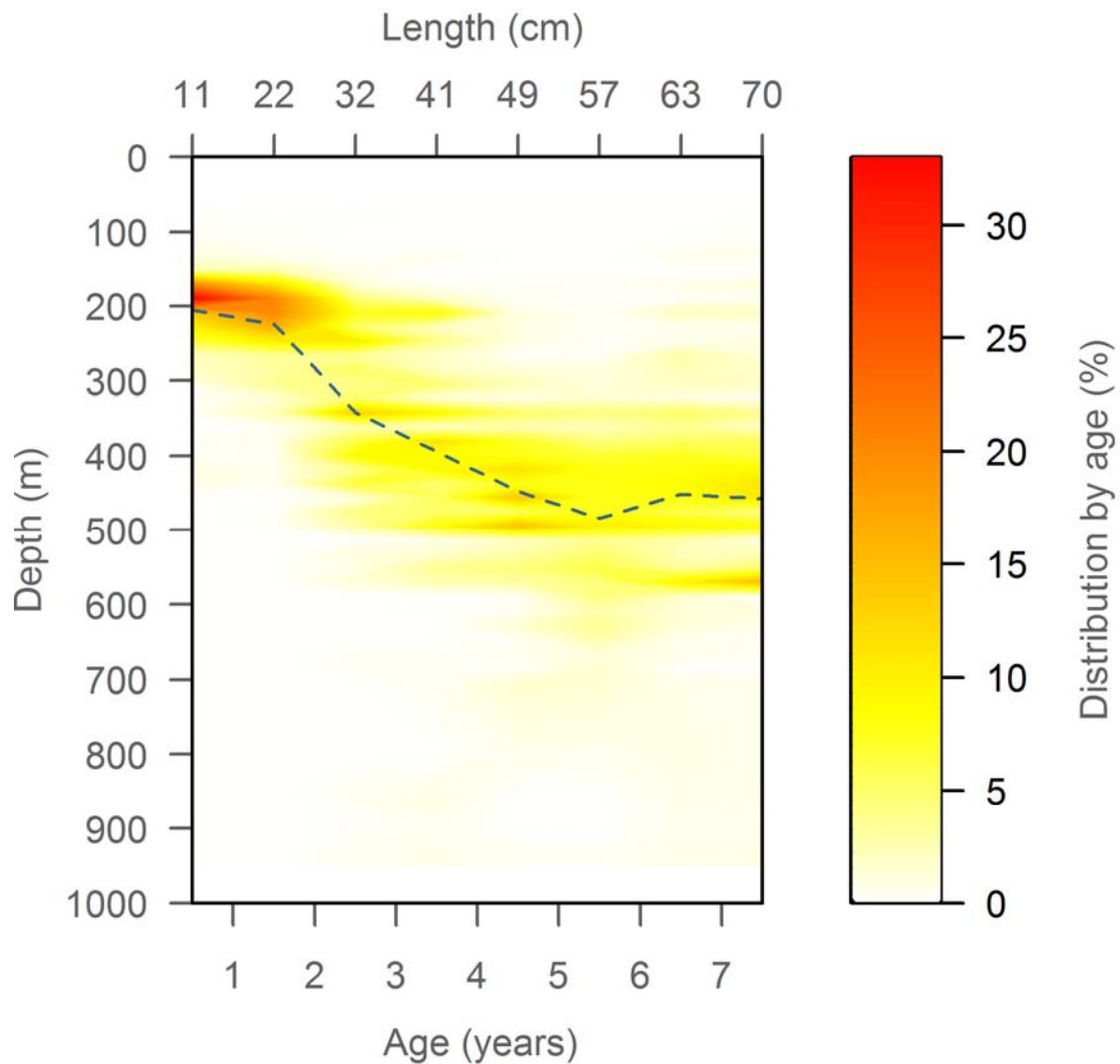
353



354

355 Figure 9. Centre of Gravity by age of deep water cape hake (*M. paradoxus*) on each side of the Orange
 356 River mouth (national border between South Africa and Namibia).

357



358

359 Figure 10. Depth distribution of deep water cape hake (*M. paradoxus*) by age and mean length. Grey
 360 dashed line indicates the mean depth.

361

362 [Excluded]

363 Figure 11. Abundance index time series of deep water cape hake (*M. paradoxus*). a) 0.5 year old
 364 (recruits). b) 1.5-2.5 year old (juveniles). c) 3.5-7.5 year old (large juveniles and adults).

365

366 Supplementary information 1. Description of the "Latent Cohort GeoPop model".

GeoPop: The latent cohort model

1 Description of the Latent Cohort GeoPop model

The model is a modification of the length-based GeoPop. The model contains two major components:

1. A model of the space-time distribution of cohorts and
2. A simple size spectrum model for each cohort.

In the following we describe the model components. Model parameters are listed in table 2.

2 Component 1 – cohort correlation

A Gaussian Markov random field was used to model log-abundance $\eta(x, t, c)$ of hake as function of space, time and cohort identifier (year class). Here we describe how the correlation structure was defined and why. Since a cohort defines a fixed group of individuals it is natural to expect that the distribution pattern of a cohort changes continuously in space and time. A simple choice of correlation structure for a given cohort c is the space time separable correlation of the form

$$\rho(\Delta x, \Delta t) = \rho(x, \Delta x)\rho(\Delta t)$$

Here Δx denotes spatial distance while Δt denotes time distance. The correlation structure states that the similarity of abundance at two space time locations (x_0, t_0) and (x_1, t_1) decays with both spatial distance $|x_0 - x_1|$ and time distance $|t_1 - t_0|$. The rates of decay are unknown and must be estimated. The decay rates describe how fast the distributional patterns change over time and how spatially aggregated the species is. In particular we use the same correlation structures as used in Kristensen et al. (2013): $\rho(x, \Delta x)$ is defined as the correlation induced by a Gaussian Markov random field, and $\rho(\Delta t)$ is an exponential decaying correlation function. (These principles are also similar to Jansen et al. (2012)). This correlation structure describes the space time dynamics of a given cohort. The model is formulated for multiple cohorts by assuming independence between cohorts. The independence assumption allows cohort c to follow a completely different spatio-temporal life history than any of the other cohorts. The overall correlation structure becomes

$$\rho(\Delta x, \Delta t, \Delta c) = \rho(x, \Delta x)\rho(\Delta t)1_{(\Delta c=0)}$$

where Δc denotes the integer distance between two year classes.

3 Component 2 – link to trawl observations

The available data are length frequencies from trawl hauls without any age measurements. Such data obviously only hold indirect information about the individual cohorts. In order to link our spatio-temporal cohort model with the observations we must formulate a model of the size distribution of cohorts. For simplicity

it is assumed that the size distribution of cohort c at time t of age $a = t - c$ is given by a Gaussian density with a mean determined by a von bertalanffy growth curve and a standard deviation that increase linearly with time:

$$f_c(s, t) = \frac{1}{\sqrt{2\pi\sigma_a^2}} \exp\left(-\frac{1}{2} \frac{(s - \mu_a)^2}{\sigma_a^2}\right)$$

where $\mu_a = L_\infty(1 - \exp(-k \cdot a))$ and $\sigma_a = \alpha + \beta \cdot a$. We define the haul specific cohort strength $w_c(x, t)$ as affected by the following contributions:

1. Cohort recruitment strength $\log r(c)$ which is assumed to be a normal random effect.
2. Cohort age a and mortality z .
3. The spatial distribution $\eta(x, t, c)$ of the cohort, and
4. Small scale space-time variations in cohort strength $\eta_0(x, t, c)$ - the nugget effect:

$$\log w_c(x, t) = \log r(c) - z \cdot t + \eta(x, t, c) + \eta_0(x, t, c)$$

The observed size distribution in a spatial point x at time t is an aggregation of all cohort size distributions in the particular spatial point:

$$\lambda(s, x, t) = \sum_c w_c(x, t) f_c(s, t)$$

Finally our measurements are assumed Poisson distributed conditionally on the intensity $sel(s)\lambda(s, x, t)$ where $sel(s)$ denotes a two-parameter gear selectivity function. In case of multiple different gears, sel is extended with an overall efficiency parameter γ for each gear. The γ for the Gisund trawl was fixed to one since only relative selectivity can be estimated.

368

369 Supplementary information 2. Documentation of parameter estimation test.

370

371 Supplementary information 3. Distribution maps of deep water cape hake (*M. paradoxus*) by cohort and
372 age.

373

374 Tables

375

| Gear name | Standard trawl speed (knots) | Constraining rope | Door spread (m) | Sweep lengths (m) | Wing spread (m) | Headline height (m) | Mesh size in codend (mm) |
|--------------|------------------------------|-------------------|-----------------|-------------------|-----------------|---------------------|--------------------------|
| Gisund | 3.0 | Yes | 50 | 40 | 21 | ? | 10 |
| Old Africana | 3.5 | No | ? | 50 | 26 | 1.7 – 4.4 | 35 |
| New Africana | 3.5 | No | ? | 9 | 24.1 – 29.2 | 2.8 – 4.8 | 35 |

376

377 Table 1. Specifications of the bottom trawl gears.

378

| Symbol | Description | Unit | Estimate | Mean of estimates from bootstrap | Standard error |
|-----------------------|--------------------------------------------------|--------------------|----------|----------------------------------|----------------|
| ℓ_{50}^{Gisund} | Fish size at half selection (Gisund) | cm | ... | ... | ... |
| $\ell_{50}^{SA_New}$ | Fish size at half selection (SA_New) | cm | ... | ... | ... |
| $\ell_{50}^{SA_Old}$ | Fish size at half selection (SA_Old) | cm | ... | ... | ... |
| SR^{Gisund} | Selection range (Gisund) | cm | ... | ... | ... |
| SR^{SA_New} | Selection range (SA_New) | cm | ... | ... | ... |
| SR^{SA_Old} | Selection range (SA_Old) | cm | ... | ... | ... |
| γ_{SA_New} | Gear efficiency factor (SA_New vs. Gisund) | 1 | ... | ... | ... |
| γ_{SA_Old} | Gear efficiency factor (SA_Old vs. Gisund) | 1 | ... | ... | ... |
| N_0 | Mean recruitment | #/year | ... | ... | ... |
| $\sigma_{N_0}^2$ | Recruitment variance | 1 | ... | ... | ... |
| K | Growth rate (Von Bertalanffy) | year ⁻¹ | ... | ... | ... |
| t_0 | Theoretical age at length 0 cm (Von Bertalanffy) | year | ... | ... | ... |
| \bar{Z} | Total mortality | year ⁻¹ | ... | ... | ... |
| H | Spatial decorrelation distance | km | ... | ... | ... |
| σ^2 | Spatial variance parameter | 1 | ... | ... | ... |
| σ_N^2 | Variance of the nugget effect | 1 | ... | ... | ... |

| | | | | | |
|-------------------|------------------------------------------------|--------------------|-----|-----|-----|
| T | Decorrelation time | year ⁻¹ | ... | ... | ... |
| σ_{init}^2 | Initial length variance of cohorts | 1 | ... | ... | ... |
| σ_{rate}^2 | Rate of increase in length variance of cohorts | year ⁻¹ | ... | ... | ... |

379

380 Table 2. Model parameter estimates and standard errors.

381

382 **References**

383 BCC (2012). Status of the Fishery Resources in the Benguela Current Large Marine Ecosystem. , *Report*
384 *No. 3. Benguela Current Commission. October 2012.*

385 Bloomer, P., Santos, S., Oosthuizen, C., Hoareau, T., & Klopper, A. (2009).
Hake population
386 genetics: development of microsatellite markers and screening of microsatellite locus variation in Cape
387 hakes, *Merluccius paradoxus* and *M. capensis*, from the Namibian and South African coasts. *BENEFIT*
388 *Report, University of Pretoria, South Africa.*

389 Botha, L. (1980). The biology of the Cape hake *Merluccius capensis* Cast. and *M. paradoxus* Franca. *PhD*
390 *thesis, Stellenbosch University, South Africa.*

391 Jansen, T., & et al. (In prep.). Distribution and migration of shallow-water hake (*Merluccius capensis*) in
392 the Benguela Current Large Marine Ecosystem examined with a geostatistical population model.

393 Jansen, T., & et al. (in prep). Spawning patterns of Deep-water Cape hake (*Merluccius paradoxus*) shown
394 by Gonadosomatic index (GSI). *African J. Mar. Sci.*

395 Jansen, T., Kristensen, K., Payne, M., Edwards, M., Schrum, C., & Pitois, S. (2012). Long-term
396 Retrospective Analysis of Mackerel Spawning in the North Sea: A New Time Series and Modeling
397 Approach to CPR Data. *PLoS One*, 7(6).

398 Kristensen, K., Thygesen, U. H., Andersen, K. H., & Beyer, J. E. (2013). Estimating spatial-temporal
399 dynamics of size-structured populations. *Can J Fish Aquat Sci*, 99, 1-44.

400 Le Clus, F., Henning, H., Osborne, R., & Leslie, R. W. (2005). Size-dependent spatial dynamics of deep-
401 water Cape hake *Merluccius paradoxus* density distribution on two coasts, 1990-2003. *Marine and*
402 *Coastal Management. Marine and Coastal Management, Demersal Working Group document*
403 *WG/01/05/DH:4.*

404 Lewy, P., & Kristensen, K. (2009). Modelling the distribution of fish accounting for spatial correlation and
405 overdispersion. *Canadian Journal of Fisheries and Aquatic Sciences*, 66, 1809-1820.

- 406 MFMR, & NPC (2013). 2012 Statistics. Ministry of Fisheries and Marine Resources. [www.mfmr.gov.za](http://209.88.21.36/opencms/opencms/grnnet/MFMR/Fishing_Industry/statistics.html)
407 http://209.88.21.36/opencms/opencms/grnnet/MFMR/Fishing_Industry/statistics.html (last accessed
408 22 November 2013).
- 409 Payne, A. I. L. (1989). Cape hakes. In *Oceans of life off southern Africa*. Ed. by A. I. L. Payne, and R. J. M.
410 Crawford. Vlaeberg Publishers, Cape Town, South Africa, 136-147.
- 411 Payne, A. I. L., & Punt, A. E. (1995). Biology and fisheries of South African hakes (*M. capensis* and *M.*
412 *paradoxus*). In *Hake fisheries ecology and markets*, pp. 15–47. Ed. by J. Alheit, and T. J. Pitcher. Chapman
413 & Hall, London.
- 414 Payne, A. I. L., Rose, B., & Leslie, R. W. (1987). Feeding of hake and a first attempt at determining their
415 trophic role in the South African west coast marine environment. *African J. Mar. Sci.*, 5, 471-501.
- 416 Pillar, S. C., & Wilkinson, I. S. (1995). The diet of cape hake *Merluccius capensis* on the south coast of
417 South Africa. *African J. Mar. Sci.*, 15, 225-239.
- 418 Rademeyer, R. A., & Butterworth, D. (2013). 2013 update of the South African Hake reference case
419 assessment. *FISHERIES/2013/NOV/SWG-DEM67: MARAM IWS/DEC13/Hake/P2*.
- 420 Singh, L., Yolanda, M., & Glazer, J. (2011). *Merluccius capensis* and *M. paradoxus* length at 50% maturity
421 based on histological analyses of gonads from surveys. *DAFF Branch Fisheries document*::
422 *FISHERIES/2011/JUL/SWG-DEM/33*.
- 423 Strømme, T., Lipinski, M. R., & Kainge, P. (In prep.). Description of the life cycle of deepwater hake
424 (*merluccius paradoxus* Franca, 1960), with suggestions for its possible management n a transboundary
425 scenario. *African J. Mar. Sci.*
- 426 von der Heyden, S., Lipinski, M. R., & Matthee, C. A. (2010). Remarkably low mtDNA control region
427 diversity in an abundant demersal fish. *Molecular Phylogenetics and Evolution*, 55, 1183-1188.
- 428